JOURNAL OF MAGNETIC RESONANCE **133,** 243–254 (1998)
ARTICLE NO. MN981458

In Vivo Lactate Editing with Simultaneous Detection of Choline, Creatine, NAA, and Lipid Singlets at 1.5 T Using PRESS Excitation with Applications to the Study of Brain and Head and Neck Tumors

Josh Star-Lack,*,†,[1] Daniel Spielman,* Elfar Adalsteinsson,* John Kurhanewicz,* David J. Terris,‡ and Daniel B. Vigneron†

**Lucas MRS Imaging Center, Department of Radiology, MC5488, Stanford University, Stanford, California 94305; †Magnetic Resonance Science Center, Department of Radiology, Box 1290, University of California, San Francisco, California 94143-1290; ‡Division of Otolaryngology/Head and Neck Surgery, Stanford University, Stanford, California 94305*

Received November 3, 1997; revised March 19, 1998

Two T2-independent *J*-difference lactate editing schemes for the PRESS magnetic resonance spectroscopy localization sequence are introduced. The techniques, which allow for simultaneous acquisition of the lactate doublet (1.3 ppm) and edited singlets upfield of and including choline (3.2 ppm), exploit the dependence of the in-phase intensity of the methyl doublet upon the time interval separating two inversion (BASING) pulses applied to its coupling partner after initial excitation. Editing method 1, which allows for echo times TE = n/J (n = 1, 2, 3, . . .), alters the BASING carrier frequency for each of two cycles so that, for one cycle, the quartet is inverted, whereas, for the other cycle, the quartet is unaffected. Method 2, which also provides water suppression, allows for editing for TE > $1/J$ by alternating, between cycles, the time interval separating the inversion pulses. Experimental results were obtained at 1.5 T using a Shinnar Le–Roux-designed maximum phase inversion pulse with a filter transition bandwidth of 55 Hz. Spectra were acquired from phantoms and *in vivo* from the human brain and neck. In a neck muscle study, the lipid suppression factor, achieved partly through the use of a novel phase regularization algorithm, was measured to be over 10^3. Spectra acquired from a primary brain and a metastatic neck tumor demonstrated the presence of lactate and choline signals consistent with abnormal spectral patterns. The advantages and limitations of the methods are analyzed theoretically and experimentally, and significance of the results is discussed.

Key Words: **magnetic resonance spectroscopy (MRS); *in vivo* lactate editing; point resolved spectroscopy (PRESS); RF pulse design; human tumors.**

INTRODUCTION

The detection of lactate *in vivo* using magnetic resonance spectroscopy (MRS) may aid in the diagnosis and evaluation of several disorders. Abnormal concentrations of lactate may be correlated with nonoxidative glycolysis and have been observed *in vivo* in ischemic tissue (*1–3*), brain tumors (*4–7*), and head and neck tumors (*8*). Information gained from uncoupled moieties, which include choline (Cho, 3.2 ppm), creatine (Cr, 3.0 ppm), and *N*-acetyl aspartate (NAA, 2.0 ppm), is also important and may be useful in helping to differentiate between active tumor, necrosis, and normal parenchyma in cancer studies (*4, 9–11*). In addition, signals from mobile lipids may themselves prove relevant in the study of human cancers(*12–15*).

In order to obtain reliable estimates of lactate signal intensity, the CH_3 component (1.3 ppm) must be separated from coresonant lipids. To achieve this goal, numerous editing methods, incorporating a wide range of approaches, have been proposed (*16–37*). Multiple quantum (MQ) filters (*16–25*) offer excellent lipid suppression, but, as yet, no MQ-based sequences have been developed which provide 100% retention of lactate signal intensity as well as visibility of the singlets of interest. An alternative to multiple quantum filtering is spectral editing using *J*-difference methods (*26–34*). This class of techniques requires two separate acquisitions, but has the distinction of allowing for the observation of and discrimination between coupled and uncoupled spins while, for the lactate doublet, achieving full sensitivity. Because suppression is not obtained within a single scan, difference methods are significantly more sensitive than MQ filters to motion artifacts. Nevertheless, for many applications, subtraction techniques remain effective and are expected to retain an important role due to their practicality and ease of implementation. Moreover, as shown in this paper, suppression may be enhanced through the use of a regularization algorithm which compensates for phase and frequency variations between successive excitations.

We present a family of *J*-difference lactate editing techniques for use at 1.5 T which incorporates a pair of frequency selective inversion pulses applied to the methine quartet (4.1 ppm). The techniques meet four important design criteria in that they (1) provide T2-independent singlet suppression with resilience to B1-scaling errors, (2) can be incorporated into the PRESS (*38, 39*) volume localization sequence, (3) offer arbitrary echo times for TE >= $1/J$, and (4) readily allow for the design of filters with steep transition bands that may be re-

[1] To whom correspondence should be addressed.

1090-7807/98 $25.00

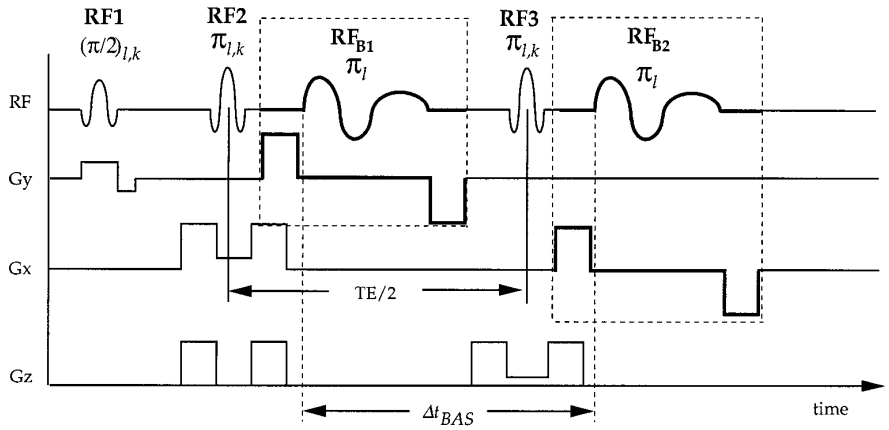

FIG. 1. Dual BASING with PRESS excitation. The time separation of the two BASING pulses (RF_{B1} and RF_{B2}) is given by Δt_{BAS}. The *l*-index refers to selectivity for the methine quartet, while the *k*-index refers to that for the methyl doublet.

quired to maintain visibility of the choline resonance. None of the previously developed methods meets all of these four criteria as techniques which depend upon selectively inverting the methyl doublet (*28*) can be sensitive to B1 errors, and techniques which depend upon applying a single inversion pulse to quartet (*26*) can be sensitive to a phase shift between the two cycles. The method introduced by Schupp *et al.* (*32*) compensated for this phase shift but only provided for an echo time of TE = 2/*J*. Item #4 above is particularly pertinent to lower field strengths such as at 1.5 T, where Cho is separated from the center of the lactate methine quartet by only 60 Hz. To our knowledge, no *J*-difference edited spectra previously have been acquired at 1.5 T allowing for the simultaneous detection of lactate as well as all singlets upfield of and including Cho.

To achieve our aims, we have utilized the dual band selective inversion with gradient dephasing (BASING) sequence (Fig. 1) which was recently introduced for solvent suppression and TE-independent lactate rephasing (*40*). BASING is similar in concept to MEGA which was developed for water suppression by Mescher *et al.* (*41*). Ross *et al.* (*42*) independently developed a *J*-difference editing technique for TE = 1/*J* using two symmetrically placed adiabatic inversion pulses surrounding one hard spin–echo (SE) pulse. The technique was applied to lactate editing of rat brains with implanted gliomas at 7 T where Cho is separated from the Lac methine quartet by 240 Hz which significantly relaxes the RF transition bandwidth design constraints compared to that required at 1.5 T. Volume selection was provided using integrated OVS–ISIS (*43*), which, unlike PRESS, is not a single shot localization technique.

Our approach is predicated upon the premise that the phase of the lactate doublet can be controlled by adjusting the time interval (Δt_{BAS}) separating the two inversion pulses applied to the methine quartet (*40*). Since it is the *relative* rather than absolute placement of these pulses that determines the intensity and sign of the absorption spectrum doublet components, this allows editing to be readily accomplished with a multi-echo localization technique such as PRESS. If desired, temporally asymmetric RF inversion waveforms (*44–46*) may be used, which, for a given amount of passband and stopband ripple, can be made to possess sharper transition bands than those associated with symmetric pulses of equal duration, thus providing a means to improve the visibility of the choline resonance while reducing RF pulse durations.

Two different schemes are presented, one for echo times TE = *n*/J (*n* = 1, 2, 3, . . .) and another, which also provides for water suppression, for arbitrary TE > 1/J + T_{min} where T_{min} is dependent upon RF and gradient timing parameters. For Scheme 1, a novel phase cycling scheme is employed which is based upon shifting the RF carrier frequency to enhance lipid suppression in the presence of B1 inhomogeneities. For Scheme 2, which is in principle insensitive to B1 scaling errors, editing is achieved by cycling Δt_{BAS}. To address problems resulting from motion-induced phase variations, we have developed a phase regularization algorithm designed to reduce cancellation artifacts. This has particular application to difficult-to-scan areas such as the neck which contain a high concentration of lipids.

This paper describes and analyzes the acquisition and processing techniques that are introduced. Experimental data acquired from phantom and *in vivo* studies at 1.5 T are shown which verify the efficacy of the techniques. These data include spectra collected from human brain, and head and neck tumors, which demonstrate abnormal intensity patterns. To our knowledge, this paper presents the first spectra containing both choline and lactate resonances acquired *in vivo* from head and neck tumors. The significance of the results and the limitations of the techniques are discussed.

METHODS

BASING for Lactate Editing

BASING comprises a frequency selective 180° pulse surrounded by B0 crusher gradients of opposite signs that cause

dephasing of flipped spins. The dual BASING implementation (Fig. 1) consists of two such pulses, with their crushers on orthogonal axes, surrounding a wideband spin–echo pulse. An important feature is that passband spin rephasing occurs independently of the BASING pulse shape so long as the two phase profiles are identical (see Eq. [2] below). Therefore, the BASING pulses need not possess linear phase to produce zero phase spectra. The effects of the pulses upon weakly coupled spins such as the lactate methine and methyl protons can be assessed using product operator theory (*47*). Emphasis will be placed on detection of the methyl doublet (1.3 ppm) due to its higher SNR and larger chemical shift separation from water.

When the methine quartet is placed within the BASING inversion band, and the PRESS spin–echo pulses are sufficiently wideband to include both the methyl doublet and the methine quartet, the in-phase doublet signal intensity M_d can be shown to be related to the time interval separating the two BASING pulses, Δt_{BAS} (Fig. 1b), in the manner

$$M_d \propto \cos(\pi J[TE - 2\Delta t_{BAS}]), \qquad [1]$$

for $\Delta t_{BAS} < TE/2$.

Equation [1] shows that Δt_{BAS} can be adjusted to rephase the doublet independently of TE and render it either *upright* or *inverted* relative to the uncoupled spins for applicability to editing. Three important cases which arise are:

(1) For all TE, the doublet will be *upright* when Δt_{BAS} is half the echo time ($\Delta t_{BAS} = TE/2$).

(2) For all $TE > 1/J$, the doublet will be *inverted* when $\Delta t_{BAS} = (TE - 1/J)/2$. In practice, the minimum echo time for complete inversion of the doublet is given by $TE_{min} = 1/J + T_{min'}$ where T_{min} is the twice the duration of the second PRESS spin–echo pulse (including crusher gradients) plus twice the duration of the BASING pulse.

(3) If neither the quartet nor the doublet is placed within the frequency selective BASING inversion band, the doublet will behave as for a conventional PRESS experiment—*upright* for $TE = n/J$, ($n = 2, 4, 6, \ldots$), and *inverted* for $TE = n/J$, ($n = 1, 3, 5, \ldots$).

The above results suggest the possibility of two editing schemes (denoted as ES-1 and ES-2), each requiring two excitations (Cycle 1 and Cycle 2):

Editing Scheme 1 *(ES-1)*—for $TE = n/J$, $n = 1, 2, 3, \ldots$ Cycle 1: The methine quartet is placed within the BASING inversion band with $\Delta t_{BAS} = TE/2$ (for n odd) and $\Delta t_{BAS} = (TE - 1/J)/2$ (for n even).

Cycle 2: The methine quartet is removed from the BASING inversion band.

Editing Scheme 2 *(ES-2)*—for $TE > 1/J + T_{min}$. The methine quartet is placed within the BASING inversion band for both cycles but the time separating the BASING pulses is changed between cycles.

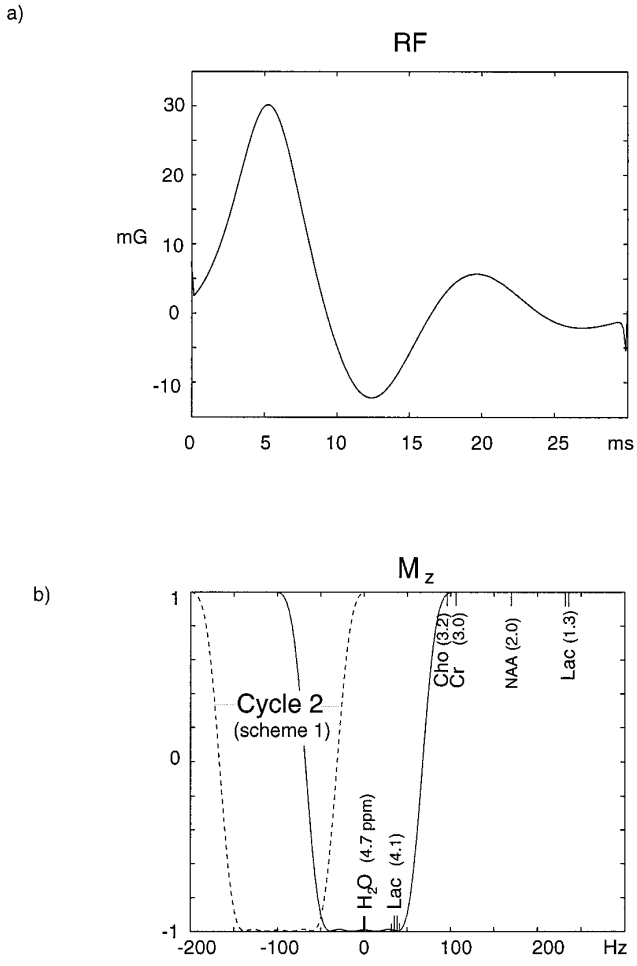

FIG. 2. (a) Maximum phase BASING highpass filter (one stopband) designed to invert the methine quartet and pass resonances upfield of Cho (3.2 ppm). (b) Inversion profile of the BASING pulse. For Editing Scheme 1 (ES-1), the Cycle 1 and Cycle 2 carrier frequencies are separated by 99 Hz.

Cycle 1: $\Delta t_{BAS} = TE/2$.

Cycle 2: $\Delta t_{BAS} = (TE - 1/J)/2$.

For both editing schemes, addition of successive Cycle 1 and Cycle 2 acquisitions yields the singlets and cancels the lactate methyl doublet, while subtraction of successive acquisitions cancels the noncoupled spins and yields the doublet. ES-1 allows for shorter echo times ($TE = 1/J$), whereas ES-2 can provide for water suppression for both cycles since the H_2O resonance (4.7 ppm) may be placed within the BASING stopband. The two schemes offer different editing sensitivities to B1 errors (see below).

RF Pulse Design

A maximum phase BASING pulse (Fig. 2) was designed using the Shinnar–LeRoux (SLR) transform (*46*, *48*, *49*), in conjunction with the Parks–McClellan (PM) FIR filter design algorithm (*50*) to generate an equiripple frequency response. The design parameters were for 1% inversion ripple and 0.1%

BASING passband ripple. The transition bandwidth of the 30-ms pulse was 55 Hz which allowed for inversion of the methine proton while passing all moieties upfield of Cho. The RF pulse design software, which runs on the MATLAB platform (MathWorks, Inc., Natick, MA), was kindly provided by Dr. John Pauly, Stanford University.

Implementation of ES-1

The BASING pulses for Cycle 2 of ES-1 were not turned off, but instead, the RF carrier frequency was shifted to move the inversion band downfield of the lactate quartet (Fig. 2b). The amount of frequency shift (99 Hz) was set to be equivalent to a multiple of the fundamental BASING passband ripple frequency generated via the PM algorithm. As shown below, this type of frequency shifting offers a means of enhancing singlet suppression.

The B1-dependent singlet suppression factor can be determined from the expression for the BASING excitation profile, which has been previously derived (*40*) using the spin–domain formalism (*46, 51*) and Cayley–Klein rotation parameters ($\alpha(\omega)$, $\beta(\omega)$) as given by

$$\alpha(\omega) = \cos\phi(\omega)/2 - in_z \sin\phi(\omega)/2,$$
$$\beta(\omega) = -i(n_x + in_y)\sin\phi(\omega)/2,$$

where ω is the chemical shift of a spin, $\phi(\omega)$ is the frequency dependent flip angle of the pulse, and the vector $\mathbf{n} = \mathbf{i}n_x + \mathbf{j}n_y + \mathbf{k}n_z$ is the axis of rotation.

Starting with initial transverse magnetization intensity M_0, the frequency-dependent excitation profile $M_{xy}^{+}(\omega)$ after application of dual BASING is

$$M_{xy}^{+}(\omega) = (\alpha_{\mathrm{BAS}}(\omega) \cdot \alpha_{\mathrm{BAS}}^{*}(\omega))^2\, \beta_{\mathrm{SE}}^{2}(\omega)\, M_0, \qquad [2]$$

where α_{BAS} refers to the two BASING pulses (assumed to be identical), and β_{SE} is the spin–echo pulse rotation parameter.

A useful figure of merit for evaluating the editing capabilities of the sequence is the reciprocal of the frequency-dependent singlet suppression factor which we denote as the attenuation factor, $\chi(\omega)$. This is calculated by dividing the difference between the Cycle 1 and Cycle 2 BASING profiles (Eq. [2]) by the nominal magnetization intensity, which is assumed to equal ${\beta_{\mathrm{SE}}}^2 M_0$ since, upfield of 3.2 ppm, α_{BAS} has a magnitude close to 1. Thus, the frequency-dependent attenuation factor is independent of β and is given by

$$\chi(\omega) \cong (\alpha_{\mathrm{CYC1}}(\omega) \cdot \alpha_{\mathrm{CYC1}}^{*}(\omega))^2 - (\alpha_{\mathrm{CYC2}}(\omega) \cdot \alpha_{\mathrm{CYC2}}^{*}(\omega))^2, \qquad [3]$$

where $\alpha_{\mathrm{CYC1}}(\omega)$ and $\alpha_{\mathrm{CYC2}}(\omega)$ are the relevant spin–domain parameters that describe the Cycle 1 and Cycle 2 BASING profiles.

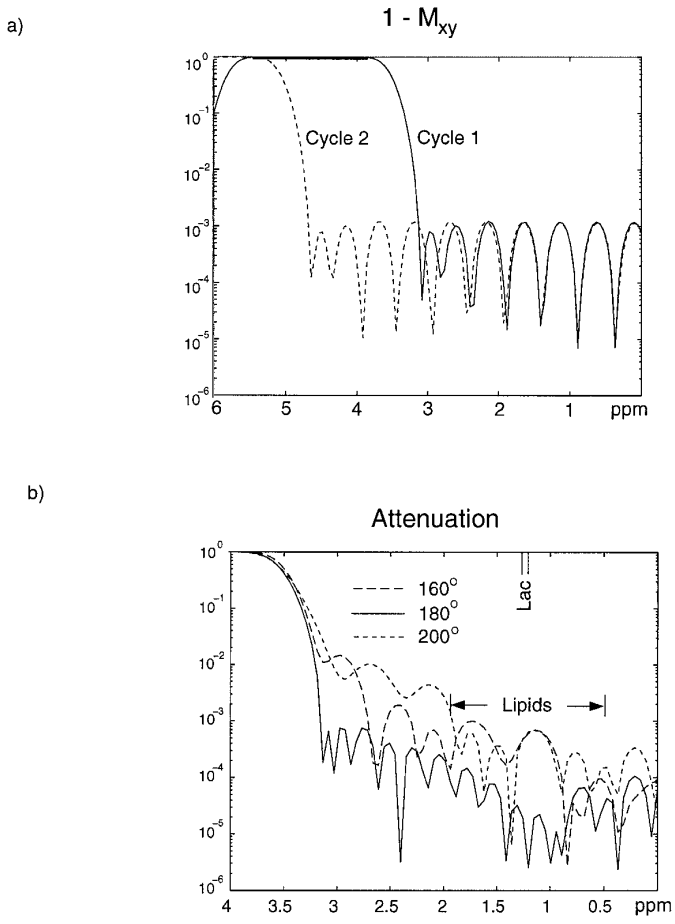

FIG. 3. Theoretical singlet attenuation factors for ES-1. (a) BASING passband ripple magnitude for Cycle 1 and Cycle 2 implementations showing overlap of the excitation profiles when the RF carrier frequency is shifted by a integral of the fundamental equiripple frequency. (b) Frequency-dependent attenuation factor $\chi(\omega)$ (Eq. [3]) for flip angles of 160°, 180°, and 200°.

By setting the amount of frequency shift between Cycle 1 and Cycle 2 to be a multiple of the fundamental ripple frequency generated using the PM algorithm, $\alpha_{\mathrm{CYC1}}(\omega)$ and $\alpha_{\mathrm{CYC2}}(\omega)$ can overlap in a constructive manner so as to improve cancellation. This can yield a theoretical lipid attenuation factor that is smaller than the design BASING passband ripple magnitude. Figure 3a shows the BASING passband ripple magnitude $1 - M_{xy}^{+}(\omega)$ for the pulse shown in Fig. 2. $M_{xy}^{+}(\omega)$ was generated using a Bloch equation simulator while assuming $\beta = 1$. It is demonstrated that a frequency shift of 99 Hz (three ripples) causes the Cycle 1 and Cycle 2 passband ripples to be well aligned within the desired suppression region (upfield of 2 ppm). The resulting singlet attenuation factor $\chi(\omega)$, given by Eq. [3], is plotted in Fig. 3b. For a perfect 180° BASING pulse, attenuation is as low as 10^{-5} near 1.3 ppm which is more than two orders of magnitude smaller than the design BASING passband ripple. The resilience of singlet suppression to RF scaling errors is also plotted.

Implementation of ES-2

Implementation of ES-2 was achieved by cycling the time position of the first BASING pulse (RF_{B1}) and associated dephasing gradients. For Cycle 1 (Δt_{BAS} = (TE/2), RF_{B1} was applied just *after* the first PRESS spin–echo pulse RF2, while for Cycle 2 (Δt_{BAS} = (TE − 1/J)/2), RF_{B1} was applied just *before* application of RF3 (for minimum echo time TE_{min}). For both cycles, the second BASING pulse (RF_{B2}) was applied just after RF3. Experimental results demonstrated a need to calibrate for a zero-order phase discrepancy associated with Cycle 1 and Cycle 2 acquisitions. This phase error, measured to be between 30° and 60°, was traced to inadequate B0-eddy current compensation that failed to properly adjust for the RF_{B1} dephasing gradients. Note that, for ES-2, α_{CYC1} is equal to α_{CYC2} independently of B1, which implies that, in principle, complete singlet suppression is achieved at all passband frequencies.

Phase Regularization

For instances when a large lipid signal was present within the PRESS volume of interest, a phase regularization routine, modeled after a method previously implemented to improve the SNR of multiacquisition (multishot) MRS experiments (*52*), was developed to improve lipid suppression. Each acquisition was individually processed so that shot-to-shot zero-order phase discrepancies and frequency shifts (both presumably motion induced) could be eliminated before final summation. This was accomplished by apodizing and Fourier transforming each FID and then automatically phasing and frequency shifting the lipid CH_2 peak of the spectrum to a chemical shift position of 1.3 ppm. Any spectra whose lipid CH_2 peak amplitude differed from the median value by more than 20% were discarded (less than 2% of the spectra were thrown away). After all the Cycle 1 and Cycle 2 acquisitions from a given experiment were processed, the data were then summed or subtracted to generate either the uncoupled or coupled spectra.

Data Acquisition

To demonstrate and evaluate the editing techniques, phantom and *in vivo* data were collected at 1.5 T using a General Electric Echo–Speed system (G.E. Medical Systems, Milwaukee, WI) equipped with self-shielded gradients (maximum magnitude = 2.2 G/cm, slew rate = 12 G/cm/ms). PRESS localization was accomplished using spatially selective SLR-designed pulses that possessed excitation profiles that were the Fourier transforms of a Hamming windowed four-lobed Sinc function (*53*). All B0 crusher gradients were of magnitude 2.0 G/cm and 4.5 ms in duration including the 250 μs rise and decay times. The time between the 90° excitation pulse and the first 180° refocusing pulse was minimized to a value of 10 ms. For all acquisitions, the receiver bandwidth was 1250 Hz and 512 points were sampled starting at echo time TE. The accumulated free induction decays (FIDs) were apodized with an exponential linebroadening filter and zero-filled to 1024 points before Fourier transformation. Baseline correction was implemented by averaging the mean value of the first and last 25 points of the phased spectra to determine the D.C. offset.

For ES-1, water suppression was achieved through the use of three CHESS (*54*) minimum phase saturation pulses (*53*), each of 60 Hz bandwidth. The flip angle of the final CHESS pulse was adjusted manually to a value between 100° and 130° to achieve optimal suppression. For ES-2, water suppression was provided by the BASING pulses.

A brain metabolite phantom (G.E. Medical Systems, Milwaukee, WI) which contained 3.0 mM Cho, 10.0 mM Cr, 12.5 mM NAA, 7.5 mM myo-Inositol (mI), 12.5 mM glutamate (Glu), and 5.0 mM lactate (Lac) was scanned with both editing schemes using a PRESS-selected volume (x, y, z) measuring $20 \times 20 \times 20$ mm^3. For the ES-1 acquisition, TE was 144 ms, whereas, for the ES-2 experiment, it was necessary to increase TE to 240 ms, thus reflecting a value of T_{min} = 96 ms. The other experimental parameters were as follows: pulse repetition time (TR) = 2 s, number of acquisitions (NA) = 60, linebroadening = 1 Hz.

In vivo data were acquired, using ES-1, from a 48-year-old female with a brain tumor diagnosed previously as a glioblastoma multiforme. The PRESS-selected region, measuring $42 \times 33 \times 26$ mm^3, was centered near the posterior corpus collosum and data were collected with the following parameters: TR = 1 s, TE = 144 ms, NA = 128.

In vivo MRS of neck tissue presents a unique challenge due to susceptibility effects, motion-induced artifacts, and increased lipid contamination. To determine an achievable lipid suppression factor, portions of the left complexus, splenius, and trapezius muscles of a normal volunteer were localized (PRESS box = $20 \times 20 \times 20$ mm^3), and data were processed both with and without the phase regularization algorithm for comparison. The potential for identifying hypoxic tumors, was investigated by acquiring spectra from a metastatic neck node of a 48-year-old man diagnosed with a primary right pyriform sinus tumor. Editing was implemented with ES-1 using the following scan parameters: TR = 2 s, TE = 144 ms, NA = 256, PRESS box = $20 \times 20 \times 20$ mm^3.

For the neck MRS experiments, data were collected using a four-element head, neck, and cervical phased-array coil (MRI Devices Corp., Waukesha, WI) operating in receive-only mode (the body coil was used to transmit). The received FIDs from each coil were individually apodized (2 Hz linebroadening), Fourier transformed, phased, and then combined in a manner designed to maximize the final SNR by scaling data from each coil by a factor proportional to that coil's measured SNR (*55*, *56*).

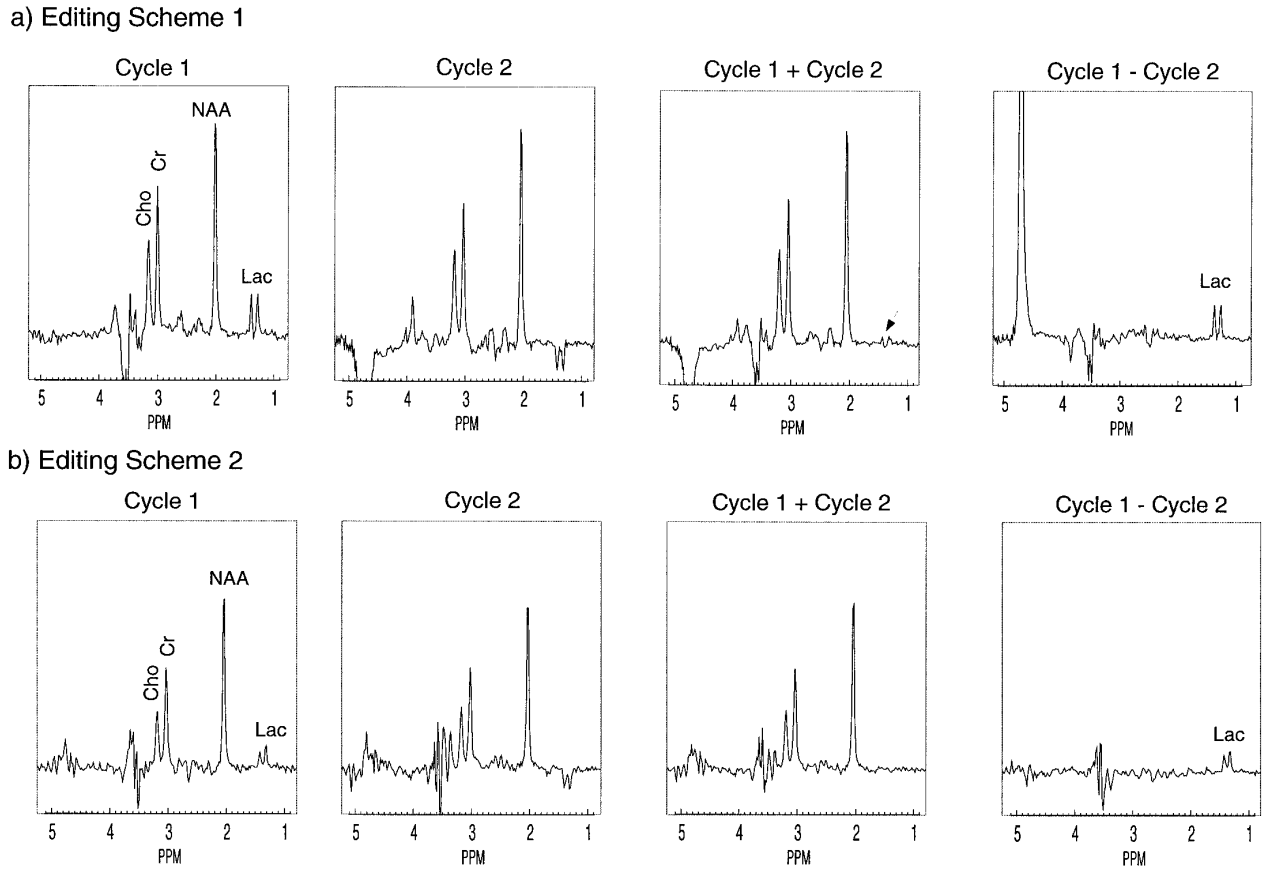

FIG. 4. Brain metabolite phantom results for (a) ES-1 (TR/TE = 2000/144) and (b) ES-2 (TR/TE = 2000/240). The ordinate scaling is identical for all displayed spectra allowing for comparison of peak intensities. Complete singlet suppression was achieved in the coupled spectra (Cycle 1 − Cycle 2), although there was minor doublet contamination in the ES-1 singlet spectrum (Cycle 1 + Cycle 2). ES-2 signal intensity was reduced due to the longer echo time.

EXPERIMENTAL RESULTS

Figure 4 shows reconstructed brain metabolite phantom spectra acquired with ES-1 (4a) and ES-2 (4b). Complete suppression of the Cho, Cr, and NAA singlets was provided by both schemes as is shown in the ''Cycle 1 − Cycle 2'' spectra. However, there was slight doublet contamination (see arrow) of the ES-1 singlet spectrum (Cycle 1 + Cycle 2) which presumably resulted from imperfections of the flip angle of the inversion pulses which were applied to the methine quartet in Cycle 1 but not in Cycle 2. Compared with ES-1, the metabolite signal intensities were reduced using ES-2 due to the echo time increase. Another difference between ES-1 and ES-2 spectra is that the residual resonances (mI, Cr, Glu) in the range of 4.0–3.5 ppm, which is in the transition band of the BASING pulse, have different profiles. Since mI and Glu contain coupled components, it is expected that the resulting lineshapes will be complicated functions of echo time, Δt_{BAS}, and the BASING excitation profile. The analysis of these lineshapes is beyond the scope of this paper. Note finally that the amount of water suppression provided by ES-2 ($>10^4$) was similar to measured BASING suppression factors that were previously reported (*40*).

The results from the brain tumor scan are displayed in Fig. 5. Figure 5a shows the outline of the PRESS box superimposed upon a T1-weighted 3-D SPGR scan (TR = 26 ms, TE = 6 ms, flip angle = 40°, 1.5 mm resolution) which was acquired after the injection of Gd-DTPA. The spectra in Fig. 5b show clear and identifiable lactate and lipid signals of similar magnitude. Although not greater than one, the ratio of Cho/NAA in the singlet spectrum (Cycle 1 + Cycle 2) was also abnormal (*57*). If a conventional PRESS scan at TE = 144 ms had been performed, the lipid and lactate signals would have almost canceled (see Fig. 5b—Cycle 2), thereby offering a misleading indicator of overall signal intensity near 1.3 ppm.

The results from the neck muscle scan of the normal volunteer are shown in Fig. 6. Reconstruction without the phase regularization algorithm yielded a lipid suppression factor of 127, which was measured by dividing the integrated peak area across the frequency range of 0.9–2.1 ppm of the ''Cycle 1 − Cycle 2'' spectrum into the integrated

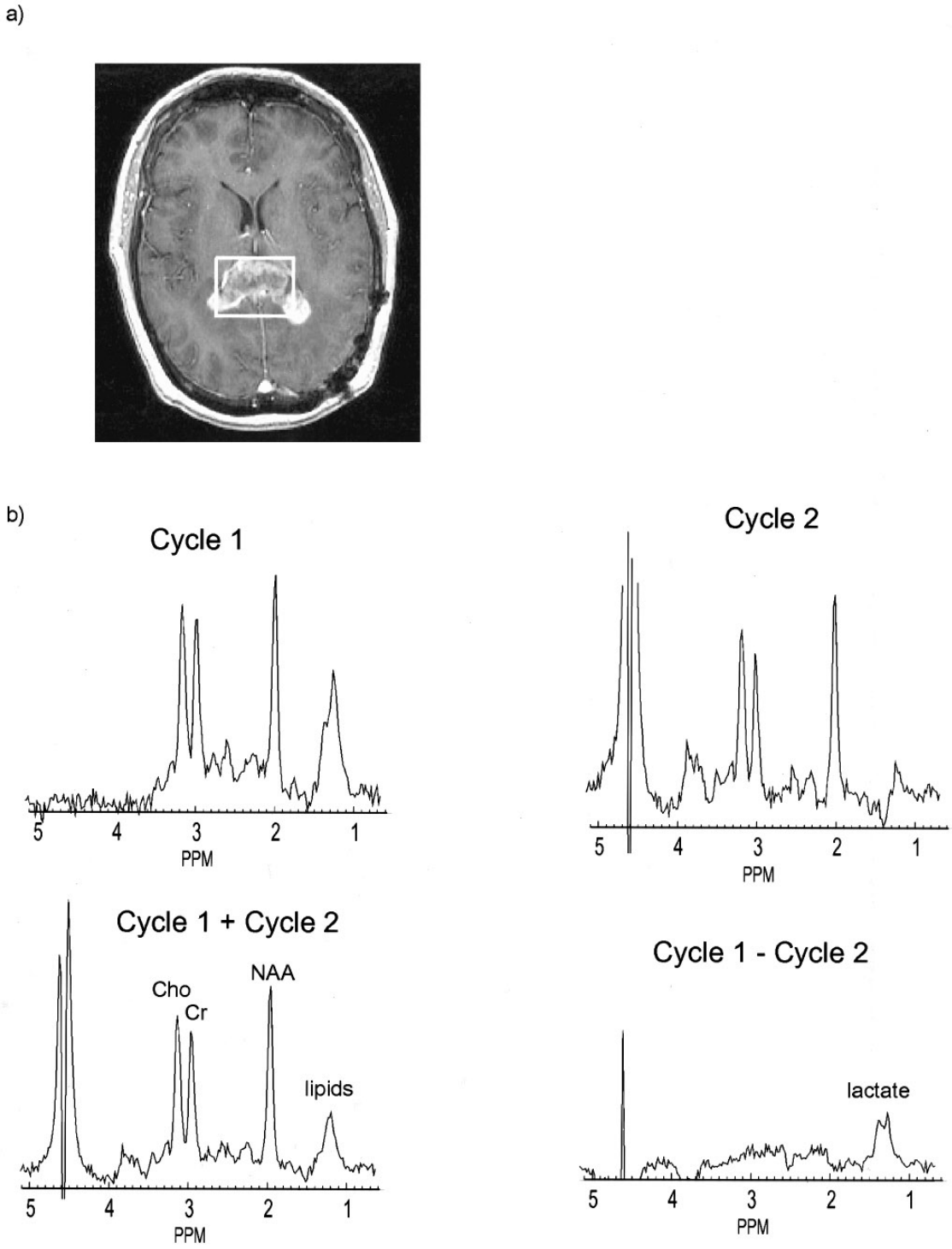

FIG. 5. Brain tumor results from a glioblastoma multiforme: (a) Postcontrast T1-weighted SPGR axial slice (TR/TE = 26/6) showing the location of the PRESS box. (b) Reconstructed spectra (TR/TE = 1000/144), each scaled identically, which indicate that similar amounts of lactate and lipids were present. The ratio of Cho to NAA was also abnormal.

area of the ''Cycle 1 + Cycle 2'' spectrum. The maximum absolute value of the ''Cycle 1 − Cycle 2'' spectrum in that region was 1/47 of the maximum lipid value. With phase regularization implemented, lipid suppression was improved to a value of over 1000, which is comparable to suppression factors that we have previously measured in phantom experiments. Note that the 3-ppm region did not experience large changes resulting from phase regularization. Here, the

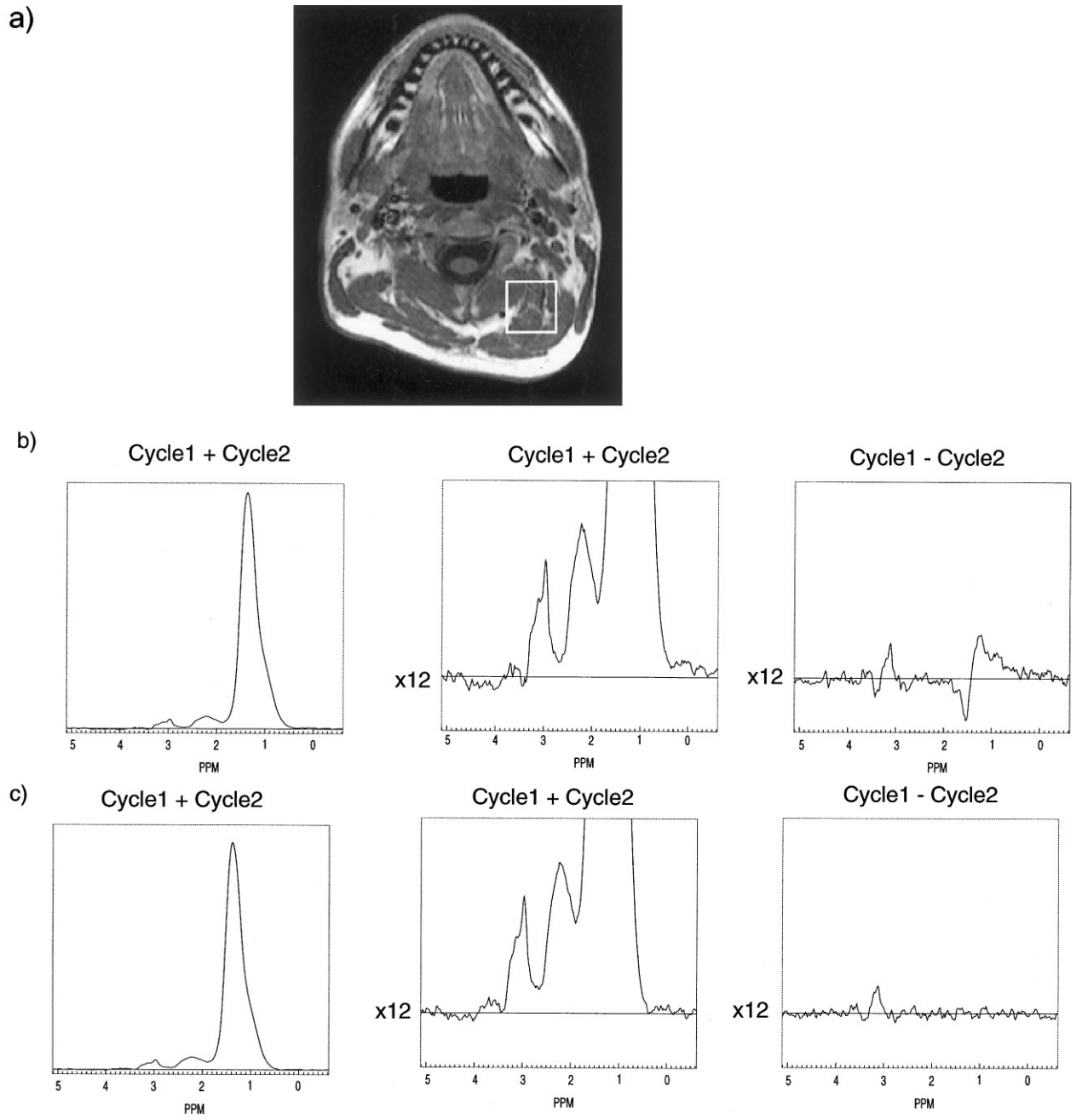

FIG. 6. Neck muscle results: (a) Axial image (TR/TE = 25/6) showing the approximate location of the PRESS box. (b, c) Spectra (TR/TE = 2000/144) reconstructed without (b) and with (c) phase regularization where the lipid suppression factor was improved to a value of over 10^3. Metabolite resonances situated near 3 ppm presumably consist of choline, creatine and carnitine moieties. The right four spectra of parts (b) and (c) are zoomed in by a factor of 12.

singlet intensities (presumably composed of choline, creatine, and carnitine) were similar in both Figs. 6a and 6b. There were also residual ''Cycle 1 − Cycle 2'' signals in the 3 ppm region which may indeed contain elements of coupled moieties or may reflect incomplete singlet cancellation due to the presence of the transition band of the BASING pulse.

Figure 7 shows the results from the MRS exam of the head and neck tumor patient. Due to the size of the node, the 8 cm^3 PRESS-selected volume could be positioned so that sampled lipid signals were significantly reduced compared with those in the muscle scan of the normal volunteer. Given the low amounts of lipids, the phase regularization algorithm was not utilized. The reconstructed spectra show that there was a pronounced singlet peak in the Cho region (3.2 ppm) as well as similar amounts of

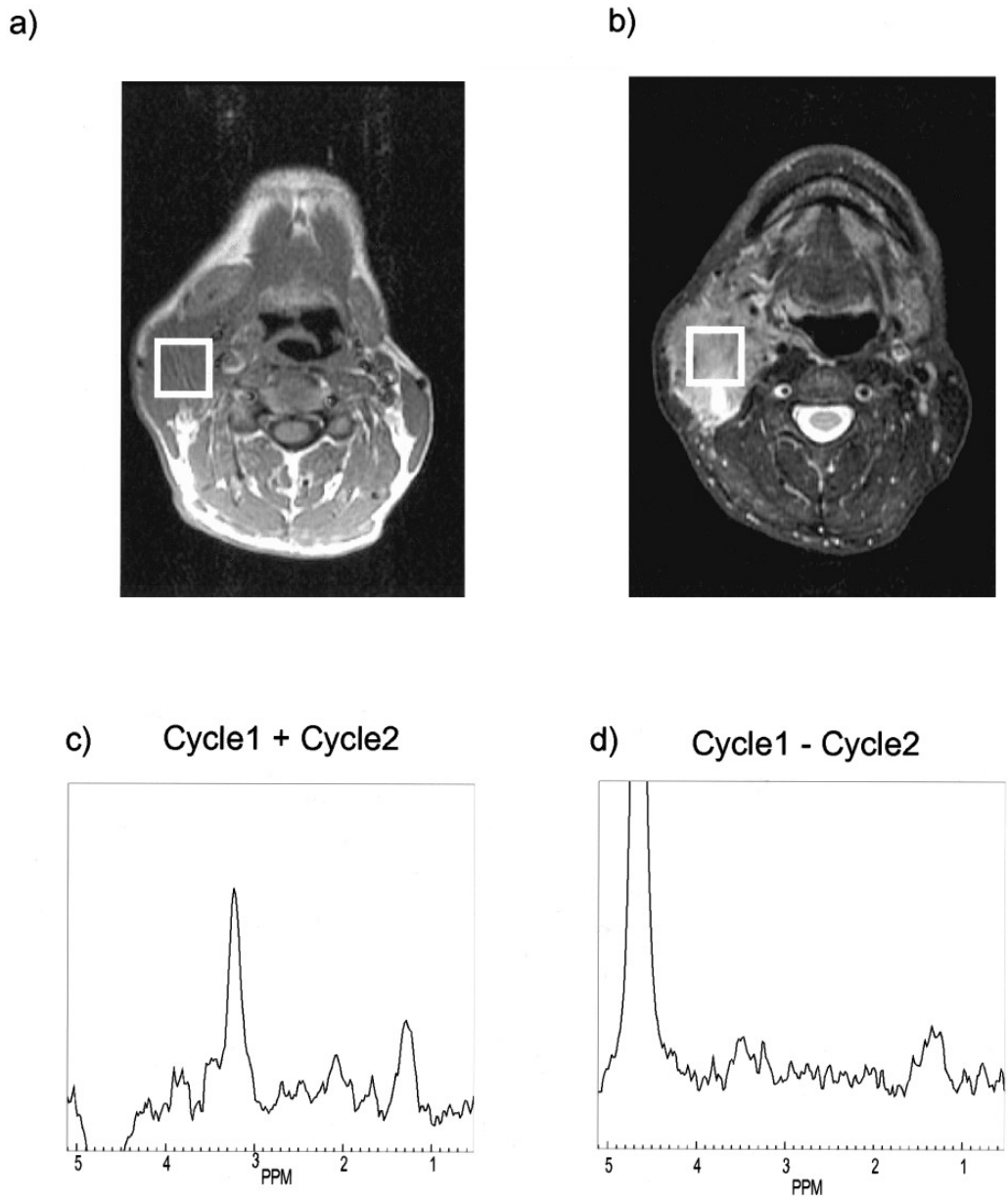

FIG. 7. Neck tumor results: (a) T1-weighted (TR/TE = 500/8) and (b) T2-weighted (TR/TE = 3000/85) axial spin–echo images (resolution = 256 × 160, FOV = 21 cm, slice thickness = 5 mm) showing the location of the PRESS box. (c, d) Edited spectra (TR/TE = 2000/144), scaled identically, showing similar amounts of lipids and lactate as well as a pronounced singlet (Cycle 1 + Cycle 2) resonance in the Cho region.

lipids and lactate. Since the sampled volume contained no muscle tissue, but only elements of the nodal mass as indicated by the hyperintensity on the T2-weighted MRI scan (Fig. 7b), the large 3.2-ppm signal, assuming it is choline, may be a marker for the presence of active tumor (*11*). The significance of the apparent lactate signal is addressed in the next section.

DISCUSSION

The experimental results demonstrate that dual BASING may be used to edit for lactate while achieving a high degree of lipid suppression. The two editing schemes presented offer different features. ES-1 allows for shorter echo times but requires additional (e.g., CHESS) water suppression and more attention to issues relating to B1 inhomogeneities since the spectral domain excitation profiles for Cycle 1 and Cycle 2 can differ. ES-2 offers both water suppression and, in principle, complete B1-insensitive singlet suppression since the chemical shift profile of the BASING pulses is the same for both cycles. However, the longer echo times may reduce the SNR and it was noticed that a phase discrepancy

between Cycle 1 and Cycle 2 acquisitions needed to be addressed.

A novel aspect of the implementation of ES-1 was the use of an inversion pulse with a equiripple excitation profile coupled with carrier frequency shifting between cycles. Aside from allowing for attenuation factors which are less than the BASING passband ripple magnitude, resilience of suppression to B1-scaling errors is also offered. As is shown in Fig. 3b, for scaling errors resulting in flip angles of 160° and 200°, the theoretical lipid attenuation factor remains less than 10^{-3} upfield of 2.0 ppm. This amount of achievable suppression is in agreement with experimental results and represents more than an order of magnitude improvement over that reported using a complementary *J*-difference technique which cycles between a wideband and narrowband spin–echo pulse applied to the lactate doublet (*33*). A disadvantage of dual BASING editing is that, since the lactate methine quartet is inverted twice, the signal intensity of the methyl doublet is more sensitive to B1 scaling errors.

Compared with ES-1, ES-2 provides for arbitrary echo times TE >= TE_{min} where $TE_{min} > 1/J$. Despite the metabolite SNR reduction that may occur, these longer echo times may be desired in some cases to help reduce lipid contamination since the metabolites tend to possess larger T2 values than lipids (*58–60*). However, if preferred, there still may be means of decreasing TE_{min}. For instance, the BASING pulse shown in Fig. 2 was designed with small ripple magnitudes and transition bandwidths which could probably be increased with marginal performance degradation. This would allow for shortening of the BASING pulse, thus reducing T_{min}. Another option is to scan at higher field strengths where the BASING pulse time could be decreased and still yield an equivalent chemical shift (ppm) transition bandwidth as would a longer pulse implemented at 1.5 T. Alternatively, TE can be shortened without changing the BASING pulse so that Δt_{BAS} for Cycle 2 is less than $(TE - 1/J)/2$. Although there will be a reduction in lactate signal intensity for that cycle (see Eq. [1]), the singlets will still cancel in the coupled (Cycle 1 − Cycle 2) spectrum, thus providing full lipid suppression. For example, a reduction of TE from 240 to 200 ms using the 30-ms pulse in Fig. 2a implemented with our PRESS excitation sequence would reduce the doublet signal intensity to 57% of its original value for Cycle 2. Since there would be no lactate signal loss for Cycle 1 (where $\Delta t_{BAS} = TE/2$), the overall SNR would decrease by only 22% for a full experiment. The lipid component at 1.3 ppm of the singlet (Cycle 1 + Cycle 2) spectrum would be contaminated with some lactate signal but could be corrected.

Another issue related to implementation of ES-2 was the phase discrepancy between Cycle 1 and Cycle 2 acquisitions that was caused by time shifting of the BASING crusher gradients. Although calibration was relatively straightforward for the phantom study, a more robust solution to the problem should be investigated before *in vivo* implementation becomes practical. One simple remedy is to fix the position of the spoilers associated with the first BASING pulse (RF_{B1}) at the extrema (spoiler #1 just after RF2, and spoiler #2 just before RF3) so that only the RF pulse need be time shifted. A disadvantage of this approach is that the time duration between the BASING crushers is increased and, hence, so are the chances of signal corruption resulting from patient motion and diffusion effects. The best solution to the problem appears to be improved B0-eddy current compensation.

For both ES-1 and ES-2, the minimum echo time remains greater than or equal to $TE = 1/J$ (144 ms). Although lactate T2's in the brain have been measured to be as long as 780 ms (*60*), this may not be the case in other parts of the body. Moreover, shorter echo times may be desired to accurately measure other metabolite and lipid/macromolecule concentrations. As pointed out by a reviewer, TE for ES-1 could be reduced to below $1/J$, which, in an analogous fashion to the proposed TE reduction for ES-2 described above, would result in a reduced lactate signal for Cycle 1. In spite of this reduced lactate signal, the echo time reduction may allow ES-1 to offer a SNR that is competitive with T1-based lipid/macromolecule suppression and editing schemes (*61, 62*) while still providing suppression factors that are independent of relaxation times.

For any *J*-difference editing scheme, suppression may be compromised by motion and other instabilities. This was a more serious issue for the neck scans where it was found that shot-to-shot phase variations could be observed. Experimental data taken from neck muscle of a normal volunteer indicated that, without phase regularization, and with NA = 256, a lipid suppression factor of approximately 100 was achieved. While it was shown that this was dramatically improved using phase compensation, the amount of suppression offered without these extra corrections may still be adequate. For the neck tumor case (Fig. 6), the lipid and lactate signal intensities were roughly equivalent, indicating that a noncompensated suppression factor of 100 would be more than sufficient.

A source of future concern would be instances where the lipid SNR is not sufficient for phasing each excitation but may still be sufficiently large to corrupt the lactate spectrum. Moreover, regardless of the suppression issues, phase regularization also may be necessary to help obtain more accurate quantitative results in a multishot experiment (*52, 63*). An alternative to phasing on a lipid peak may be to phase each acquisition on a residual water resonance—an approach which will require altering the profile of the BASING pulses to allow for inversion of the quartet but only partial inversion (and, consequently, partial suppression) of water.

In general, we have no independent test to determine the actual lactate levels in the tumor scans. The brain tumor study had sufficient homogeneity to resolve a doublet resonance at 1.3 ppm. While magnetic field homogeneity across the neck node was not adequate to resolve the lactate doublet, measurements of tissue oxygenation using an Eppendorf polargraphic oxygen electrode (Kimoc, Hamburg, FRG) yielded a median

pO_2 value of 0.7 mm Hg, which is highly suggestive of hypoxia (*64*).

In summary, two related methods for B1-robust lactate editing that maintain visibility of singlets upfield of and including 3.2 ppm at 1.5 T have been demonstrated. Edited spectra were obtained *in vivo* which allowed for measurements of the methyl group signal intensity as well as the intensity of several non-coupled spins including Cho, Cr, NAA, and lipids. Future investigations will focus on targeted applications including the correlation of the measured lactate and choline signal levels with tumor hypoxia and necrosis.

ACKNOWLEDGMENTS

The authors thank Douglas A.C. Kelley for helpful discussions, and Lucas Carvajal and Tom Brosnan for the use of their display routines. The authors also thank G.E. Medical Systems for their support. This work was supported by NIH Grants CA59897, CA-48269, CA-67166, and RR-09784, and American Cancer Society Grant EDT#34.

REFERENCES

1. J. W. B. van der Sprenkel, P. R. Luyten, P. C. Van Rijen, C. A. Tulleken, and J. A. Den Hollander, Cerebral lactate detected by regional proton magnetic resonance spectroscopy in a patient with cerebral infarction, *Stroke* **19,** 1556–1560 (1988).
2. H. Bruhn, J. Frahm, M. L. Gyngell, K. D. Merboldt, W. Hanicke, and R. Sauter, Cerebral metabolism in man after acute stroke: New observations using localized proton NMR spectroscopy, *Magn. Reson. Med.* **9,** 126–131 (1989).
3. J. H. Duijn, G. B. Matson, A. A. Maudsley, J. W. Hugg, and M. W. Weiner, Human brain infarction: Proton MR spectroscopy, *Radiology* **183,** 711–718 (1992).
4. J. R. Alger, J. A. Frank, A. Bizzi, M. J. Fulham, B. X. DeSouza, M. O. Duhaney, S. W. Inscoe, J. L. Black, Z. P. van, C. T. Moonen, and G. di Chino, Metabolism of human gliomas: assessment with H-1 MR spectroscopy and F-18 fluorodeoxyglucose PET [see comments]. *Radiology* **177,** 633–641 (1990).
5. K. Herholz, W. Heindel, P. R. Luyten, J. A. Jen Hollander, U. Pietrzyk, J. Voges, H. Kugel, G. Friedmann, and W. D. Heiss, In vivo imaging of glucose consumption and lactate concentration in human gliomas, *Ann. Neurol.* **31,** 319–327 (1992).
6. H. Kugel, W. Heindel, R. I. Ernestus, J. Bunke, M. R. du, and G. Friedmann, Human brain tumors: Spectral patterns detected with localized H-1 MR spectroscopy, *Radiology* **183,** 701–709 (1992).
7. P. E. Sijens, D. P. van, and M. Oudkerk, Correlation between choline level and Gd-DTPA enhancement in patients with brain metastases of mammary carcinoma, *Magn. Reson. Med.* **32,** 549–555 (1994).
8. E. Adalsteinsson, D. M. Spielman, J. M. Pauly, D. J. Terris, G. Sommer, and A. Macovski, A feasibility study of lactate imaging of head and neck tumors, *NMR Biomed.,* in press.
9. H. Bruhn, J. Frahm, M. L. Gyngell, K. D. Merboldt, W. Hanicke, R. Sauter, and C. Hamburger, Noninvasive differentiation of tumors with use of localized H-1 MR spectroscopy in vivo: Initial experience in patients with cerebral tumors, *Radiology* **172,** 541–548 (1989).
10. J. H. Langkowski, J. Wieland, H. Bomsdorf, D. Leibfritz, M. Westphal, W. Offermann, and R. Maas, Pre-operative localized in vivo proton spectroscopy in cerebral tumors at 4.0 Tesla—First results, *Magn. Reson. Imaging* **7,** 547–555 (1989).
11. S. K. Mukherji, S. Schiro, M. Castillo, L. Kwock, K. E. Muller, and W. Blackstock, Proton MR spectroscopy of squamous cell carcinoma of the extracranial head and neck: In vitro and in vivo studies, *AJNR,* 1057–1072 (1997).
12. C. E. Mountford, L. C. Wright, K. T. Holmes, W. B. Mackinnon, P. Gregory, and R. M. Fox, High-resolution proton nuclear magnetic resonance analysis of metastatic cancer cells, *Science* **226,** 1415–1418 (1984).
13. A. C. Kuesel, G. R. Sutherland, W. Halliday, and I. C. Smith, 1H MRS of high grade astrocytomas: Mobile lipid accumulation in necrotic tissue, *NMR Biomed.* **7,** 149–155 (1994).
14. W. G. Negendank, R. Sauter, T. R. Brown, J. L. Evelhoch, A. Falini, E. D. Gotsis, A. Heerschap, K. Kamada, B. C. Lee, M. M. Mengeot, E. Moser, K. A. Padavic-Shaller, J. A. Sanders, T. A. Spraggins, A. E. Stillman, B. Terwey, T. J. Vogl, K. Wicklow, and R. A. Zimmerman, Proton magnetic resonance spectroscopy in patients with glial tumors: A multicenter study, *J. Neurosurg.* **84,** 449–458 (1996).
15. C. Remy, N. Fouilhe, I. Barba, E. Sam-Lai, H. Lahrech, M. G. Cucurella, M. Izquierdo, A. Moreno, A. Ziegler, R. Massarelli, M. Decorps, and C. Arus, Evidence that mobile lipids detected in rat brain glioma by 1H nuclear magnetic resonance correspond to lipid droplets, *Cancer Res.* **57,** 407–414 (1997).
16. C. H. Sotak, D. M. Freeman, and R. E. Hurd, The unequivocal determination of in vivo lactic acid using two dimensional double-quantum coherance-transfer spectroscopy, *J. Magn. Reson.* **78,** 382–388 (1988).
17. C. H. Sotak and D. M. Freeman, A method for volume-localized lactate editing using zero-quantum coherence created in a stimulated-echo pulse sequence, *J. Magn. Reson.* (1988).
18. A. Knuttel and R. Kimmich, Double-quantum filtered volume-selective NMR spectroscopy, *Magn. Reson. Med.* **10,** 404–410 (1989).
19. G. C. McKinnon and P. Bosiger, Localized double-quantum filter and correlation spectroscopy experiments, *Magn. Reson. Med.* **6,** 334–343 (1988).
20. R. E. Hurd and D. M. Freeman, Metabolite specific proton magnetic resonance imaging, *Proc. Natl. Acad. Sci. USA* **86,** 4402–4406 (1989).
21. L. A. Trimble, J. F. Shen, A. H. Wilman, and P. S. Allen, Lactate editing by means of selective-pulse filtering of both zero and double-quantum coherence signals, *J. Magn. Reson.* **86** (1990).
22. Q. He, D. C. Shungu, P. C. van Zijl, Z. M. Bhujwalla, and J. D. Glickson, Single-scan in vivo lactate editing with complete lipid and water suppression by selective multiple-quantum-coherence transfer (Sel-MQC) with application to tumors, *J. Magn. Reson. B* **106,** 203–211 (1995).
23. A. H. Wilman, M. Astridge, R. E. Snyder, and P. S. Allen, Same-scan acquisition of both edited J-coupled multiplets and singlet resonances of uncoupled spins for proton MRS, *J. Magn. Reson. B* **109,** 202–205 (1995).
24. Q. He, Z. M. Bhujwalla, and J. D. Glickson, Proton detection of choline and lactate in EMT6 tumors by spin-echo-enhanced selective multiple-quantum-coherence transfer, *J. Magn. Reson. B* **112,** 18–25 (1996).
25. L. Jouvensal, P. G. Carlier, and G. Bloch, Practical implementation of single-voxel double-quantum editing on a whole-body NMR spectrometer: Localized monitoring of lactate in the human leg during and after excercise, *Magn. Reson. Med.* **36,** 487–490 (1996).
26. D. L. Rothman, K. L. Behar, H. P. Hetherington, and R. G. Shulman, Homonuclear 1H double-resonance difference spectroscopy of the rat brain in vivo, *Proc. Natl. Acad. Sci. USA* **81,** 6330–6334 (1984).

27. H. P. Hetherington, M. J. Avison, and R. G. Shulman, 1H homonuclear editing of rat brain using semiselective pulses, *Proc. Natl. Acad. Sci. USA* **82,** 3115–3118 (1985).

28. S. R. Williams, D. G. Gadian, and E. Proctor, A method for lactate detection *in vivo* by spectral editing without the need for double irradiation, *J. Magn. Reson.* **66,** 562–567 (1986).

29. C. C. Hanstock, M. R. Bendall, H. P. Hetherington, D. P. Boisvert, and P. S. Allen, Localized *in vivo* proton spectroscopy using depth-pulse spectral editing, *J. Magn. Reson.* **71,** 349–354 (1987).

30. T. Jue, Two for one: Simultaneously winnowing the ^{13}C–^{1}H and ^{12}C–^{1}H signals using only ^{1}H pulses, *J. Magn. Reson.* **73,** 524–529 (1987).

31. H. P. Hetherington, J. R. Hamm, J. W. Pan, D. L. Rothman, and R. G. Shulman, A fully localized ^{1}H homonuclear editing sequence to observe lactate in the human skeletal muscle after exercise, *J. Magn. Reson.* **82,** 86–96 (1989).

32. D. G. Schupp, H. Merkle, J. M. Ellerman, Y. Ke, and M. Garwood, Localized detection of gliomay glycolysis using edited ^{1}H MRS, *Magn. Reson. Med.* **30,** 18–27 (1993).

33. E. Adalsteinsson, D. M. Spielman, G. A. Wright, J. M. Pauly, C. H. Meyer, and A. Macovski, Incorporating lactate/lipid discrimination into a spectroscopic imaging sequence, *Magn. Reson. Med.* **30,** 124–130 (1993).

34. D. C. Shungu and J. D. Glickson, Band-selective spin echoes for in vivo localized 1H NMR spectroscopy, *Magn. Reson. Med.* **32,** 277–284 (1994).

35. R. Reddy, V. H. Subramanian, B. J. Clark, and J. S. Leigh, Longitudinal spin-order-based pulse sequence for lactate editing, *Magn. Reson. Med.* **19,** 477–482 (1991).

36. D. Bourgeois and P. Kozlowski, A highly sensitive lactate editing technique for surface coil spectroscopic imaging in vivo, *Magn. Reson. Med.* **29,** 402–406 (1993).

37. M. Bunse, W. Jung, F. Schick, G. J. Dietze, and O. Lutz, HOPE, a new lactate editing method, *J. Magn. Reson. B* **109,** 270–274 (1995).

38. R. J. Ordidge, M. R. Bendall, R. E. Gordon, and A. Connelly, *in* ''Magnetic Resonance in Biology and Medicine'' (Govil, Khetrapal, Saran, Eds.), p. 387, Teta McGraw–Hill, New Dehli, India (1985).

39. P. A. Bottomley, Spatial localization in NMR spectroscopy in vivo, *Ann. N.Y. Acad. Sci.* **508,** 333–348 (1987).

40. J. Star-Lack, S. J. Nelson, J. Kurhanewicz, L. R. Huang, and D. B. Vigneron, Improved water and lipid suppression for 3-D PRESS CSI using RF band selective inversion with gradient dephasing (BASING), *Magn. Reson. Med.* **38,** 311–321 (1997).

41. M. Mescher, A. Tannus, O. Johnson, and M. Garwood, Solvent suppression using selective echo dephasing, *J. Magn. Reson. A* **123,** 226–229 (1996).

42. B. D. Ross, T. L. Chenevert, E. R. Neal, O. Ben-Yoseph, and M. Garwood, Assessment of early metabolic changes following BCNU treatment of experimental intracerebral gliomas using localized ^{1}H MRS, *in* ''Proceedings of the ISMRM Fourth Scientific Meeting,'' New York, 374 (1996).

43. R. A. de Graaf, Y. Luo, M. Terpstra, H. Merkle, and M. Garwood, A new localization method using an adiabatic pulse, BIR-4, *J. Magn. Reson. B* **106,** 245–252 (1995).

44. S. Conolly, D. Nishimura, and A. Macovski, Optimal control solutions to the magnetic resonance selective excitation problem, *IEEE Trans. Med. Imaging* **MI-5,** 106–115 (1986).

45. J. B. Murdoch, A. H. Lent, and M. R. Kritzer, Computer-optimized narrowband pulses for multislice imaging, *J. Magn. Reson.* **74,** 226–263 (1987).

46. J. Pauly, P. Le. Roux, D. Nishimura, and A. Macovski, Parameter relations for the Shinnar Le-Roux RF design algorithm, *IEEE Trans. Med. Imaging* **10,** 53–65 (1991).

47. O. W. Sorenson, G. W. Eich, and R. R. Ernst, Product operator formalism for the description of NMR pulse experiments, *Prog. NMR Spectrosc.* **16,** 163–192 (1983).

48. P. Le Roux, Exact synthesis of radio frequency waveforms, *in* ''Proceedings, SMRM, 7th Annual Meeting, ''San Francisco 1049 (1988).

49. M. Shinnar, S. Eleff, H. Subramanian, and J. S. Leigh, The synthesis of pulse sequences yielding arbitrary magnetization vectors, *Magn. Reson. Med.* **12,** 74–80 (1989).

50. A. V. Oppenheim, and R. W. Schafer, ''Discrete Time Signal Processing,'' Prentice Hall, Englewood Cliffs, NJ (1989).

51. E. T. Jaynes, Matrix treatment of nuclear induction, *Phys. Rev.* **74,** 226–263 (1955).

52. G. Zhu, D. Gheorghiu, and P. S. Allen, Motional degradation of metabolite signal strengths when using STEAM: A correction method, *NMR Biomed.* **5,** 209–211 (1992).

53. P. G. Webb, N. Sailasuta, S. J. Kohler, T. Raidy, R. A. Moats, and R. E. Hurd, Automated single-voxel proton MRS: Technical development and multisite verification, *Magn. Reson. Med.* **169,** 207–212 (1994).

54. A. Haase, J. Frahm, W. Hanicke, and D. Matthaei, 1H NMR chemical shift selective (CHESS) imaging, *Phys. Med. Biol.* **30,** 341–344 (1985).

55. P. B. Roemer, W. A. Edelstein, C. E. Hayes, S. P. Souza, and O. M. Mueller, The NMR phased array, *Magn. Reson. Med.* **16,** 192–225 (1990).

56. L. L. Wald, S. E. Moyher, M. R. Day, S. J. Nelson, and D. B. Vigneron, Proton spectroscopic imaging of the human brain using phased array detectors, *Magn. Reson. Med.* **34,** 440–445 (1995).

57. S. J. Nelson, M. R. Day, L. Carvajal, S. E. Moyher, D. Meaney, R. Henry, L. L. Wald, and D. B. Vigneron, Methods for analysis of serial volume MRI and ^{1}H MRS data for the assessment of response to therapy in patients with brain tumors, *in* ''Proceedings, SMR, 3rd Annual Meeting,'' Nice, France, 1960 (1995).

58. J. Frahm, H. Bruhn, M. L. Gyngell, K. D. Merboldt, W. Hanicke, and R. Sauter, Localized proton NMR spectroscopy in different regions of the human brain in vivo. Relaxation times and concentrations of cerebral metabolites, *Magn. Reson. Med.* **11,** 47–63 (1989).

59. R. Kreis, N. Farrow, and B. D. Ross, Localized 1H NMR spectroscopy in patients with chronic hepatic encephalopathy. Analysis of changes in cerebral glutamine, choline and inositols, *NMR Biomed.* **4,** 109–116 (1991).

60. A. M. Blamire, G. D. Graham, D. L. Rothman, and J. W. Prichard, Proton spectroscopy of human stroke: Assessment of transverse relaxation times and partial volume effects in single volume steam MRS, *Magn. Reson. Imaging* **12,** 1227–1235 (1994).

61. D. M. Spielman, J. M. Pauly, A. Macovski, G. H. Glover, and D. R. Enzmann, Lipid-suppressed single- and multisection proton spectroscopic imaging of the human brain, *J. Magn. Reson. Imaging* **2,** 253–262 (1992).

62. J. H. Hwang, G. D. Graham, K. L. Behar, J. R. Alger, J. W. Prichard, and D. L. Rothman, Short echo time proton magnetic resonance spectroscopic imaging of macromolecule and metabolite signal intensities in the human brain, *Magn. Reson. Med.* **35,** 633–639 (1996).

63. S. Posse and D. Le Bihan, Motion artifact compensation for 1H spectroscopic imaging by signal tracking, *J. Magn. Reson. B* **102,** 222–227 (1993).

64. D. J. Terris and E. P. Dunphy, Oxygen tension measurements of head and neck cancers, *Arch. Otolaryngol Head Neck Surg.* **120,** 283–287 (1994).